Int J Adv Manuf Technol (2016) 83:1583–1593
DOI 10.1007/s00170-015-7686-x

ORIGINAL ARTICLE

Effects of filling status of cold wire on the welding process stability in twin-arc integrated cold wire hybrid welding

T. Xiang[1] · H. Li[1] · H. L. Wei[1] · Y. Gao[2]

Received: 28 March 2015 / Accepted: 3 August 2015 / Published online: 18 August 2015

Abstracts Twin-wire metal inert gas/metal active gas (MIG/MAG) arc welding is one typical type of the high-efficient welding technologies. In order to further improve the welding efficiency without increasing the welding heat input, a novel welding technology entitled twin-arc integrated cold wire hybrid welding was developed. The addition of cold wire not only increased the welding deposition rate but also improved the welding stability. In this paper, the influential mechanism of cold wire on welding stability was studied by the high-speed photography and electrical signal acquisition. It was found that the cathode spot could be stabilized on the surface of the weld pool by increasing the cold wire feed speed, which significantly improved the welding stability. The main reasons are as follows: the addition of cold wire significantly decreased the temperature of the liquid weld pool metal around the cold wire. This led to increasing the electron emission difficulty and reducing the gradient distribution of surface tension. Therefore, the cathode spot would be more likely to stabilize in the high temperature zone instead of drifting with the rear flow of the liquid weld pool metal. Besides, the cathode spot could also be stabilized because of the less dramatic fluid flow of the liquid metal. Finally, the welding stability was evaluated by a mathematical statistic method, which further verified that the welding stability could be improved with the increase of cold wire feed speed to a proper range.

Keywords Twin-arc integrated cold wire hybrid welding · Cathode spot · Welding stability · Arc coupling area

✉ H. L. Wei
weihuiliang@tju.edu.cn

T. Xiang
xiangting123@tju.edu.cn

H. Li
lihuan@tju.edu.cn

Y. Gao
gaoying@tju.edu.cn

[1] Tianjin Key Laboratory of Advanced Joining Technology, Tianjin University, Tianjin 300072, China

[2] Tianjin key Laboratory of High Speed Cutting and Precision Machining, Tianjin University of Technology and Education, Tianjin 300222, China

1 Introduction

In recent years, with a variety of products, structures, materials, and conditions, not only are welding quality requirements more and more high but also welding workload increases gradually. In order to cope with these requirements, the high-efficient welding technology has been already taken more seriously [1]. Taking gas metal arc welding (GMAW), for example, a great deal of research efforts that are mainly in respect of multi-wire arc welding equipped with single or several welding power sources were carried out [2–4]. Corresponding welding technologies were developed, e.g., tandem twin-wire welding [5–7], consumable double-electrode GMA welding [8–11], hybrid laser double GMA welding [12–14], etc.

The twin-wire metal inert gas/metal active gas (MIG/MAG) welding has been more and more mature gradually. How to further improve the welding efficiency has become the concerned question [15, 16]. Considering about the double-arc coupling effect of twin-wire welding process, the welding efficiency can be further increased with the constant heat input by increasing the number of wires (no arcing) without additional arc introduced.

Based on the above consideration, the advanced three-electrode MAG welding was developed by CLOOSE [17,

18]. In the advanced three-electrode welding process, a filler wire was added as the third electrode between the leading and trailing consumable electrodes. The leading and trailing electrodes that could perform a positional shift around its own axis of rotation were design as a straight line. Furthermore, the addition of the filler wire cooled down the weld pool, which resulted in higher liquid metal viscosity and better weld bead. But these electrodes were placed in three welding torches supplied by the two welding power sources. This led to the absence of communication between two arcs, good arc controllability and accurate control over the wires melting and metal transfer. Moreover, the integrated cold wire (ICE™) submerged arc welding (SAW) was developed by ESAB [19]. Three wires were integrated in a single welding torch, and the cold wire was parallelly arranged between the two molten wires and mainly melted by the excess arc heat, which significantly increased the welding efficiency and reduced the flux consumption and deformation. Compared with twin-wire SAW, the deposition rate for the integrated cold wire submerged arc welding can increase about 26 % by feeding the cold wire. However, this technology is only applied in the field of SAW rather than in the field of GMAW.

Based on the prior researches, this paper proposed a novel high-efficient welding technology entitled twin-arc integrated cold wire hybrid welding. In practical welding process, three wires arranged into an equilateral triangle were integrated in a single welding torch. The two consumable electrodes melted the base metal ahead while the cold wire was directly fed into the weld pool and mainly melted by the heat from the weld pool, as shown in Fig. 1. The two consumable electrodes were respectively supplied by the two welding power sources that could provide the pulse modes of multiple phase relationships through the communication with each other. In addition, the weld pool was fully stirred by the periodic pulse current, which could refine grains and improve the mechanical properties of weld bead. It was realizable to control the arc interaction, arcing time, heat distribution of the weld pool, etc.

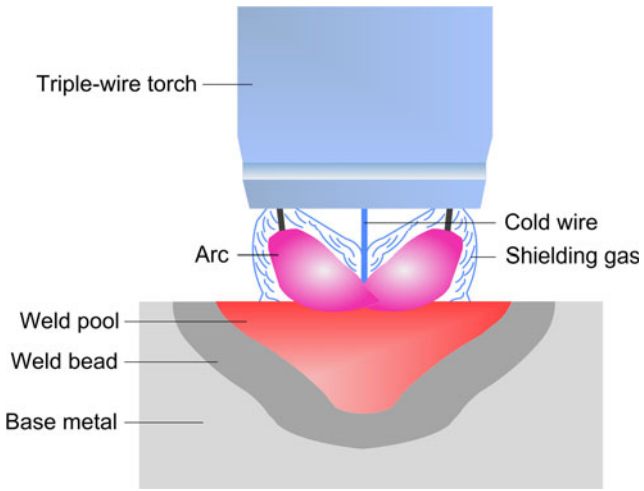

Fig. 1 Welding mechanism of twin-arc integrated cold wire hybrid welding

It is generally known that there are two main methods to increase the welding efficiency. One is increasing the deposition rate, and the other is increasing the welding speed. A novel technology entitled twin-arc integrated cold wire hybrid welding put emphasis on the latter, i.e., increasing the deposition rate, and the stable welding process would be carried out at the deposition rate of 7.476 kg/h. While all of the welding parameters kept constant, the deposition rate for the twin-wire GMAW only reached 6.097 kg/h. Compared with the twin-wire GMAW, the deposition rate for the twin-arc integrated cold wire hybrid welding has increased about 23 %. Besides, the deposition rate for the twin-arc integrated cold wire hybrid welding can reach 7.476 kg/h when the heat input kept about 24 kJ/cm. While the heat input kept constant (24 kJ/cm), the deposition rate for the twin-wire GMAW can only reach 6.097 kg/h. Thus, the deposition rate can be increased by adding the cold wire while the heat input kept constant, and the deposition rate would increase with the increase of cold wire feed speed. Besides, the dilution would decrease from 33.81 to 25.44 % with the increase of cold wire feed speed, and the dilution in twin-wire GMAW was about 34.61 %. Compared with the twin-wire GMAW, the dilution in twin-arc integrated cold wire hybrid welding can be adjusted by changing the cold wire feed speed.

As is known to all, the addition of cold wire contributes to increasing the deposition rate while the heat input kept constant. But, the effect of cold wire on welding process stability has never been studied. This paper is not just for introducing a novel high-efficient welding technology but also for studying the influential mechanism of cold wire on welding process.

2 Experimental system

The experimental system of the twin-arc integrated cold wire hybrid welding established in this study is illustrated in Fig. 2. Three electrodes were integrated in a single welding torch and arranged into an equilateral triangle in the same circle. In order to gather together arcs to form a single welding pool, the three electrodes that were bent towards the center axis of welding torch formed a 7° angle relative to the central axis of welding torch. Three electrodes were isolated to each other and equipped with independent shielding gas and cooling water channels. In this way, it could serve as both good gas protective effect to reduce welding defects and good cooling effect of welding torch to ensure service life.

In practical welding, the base metal was heated and melted by the energy from arcs between the two consumable electrodes and the workpiece. The cold wire was directly fed into the weld pool and mainly melted by the heat from the weld

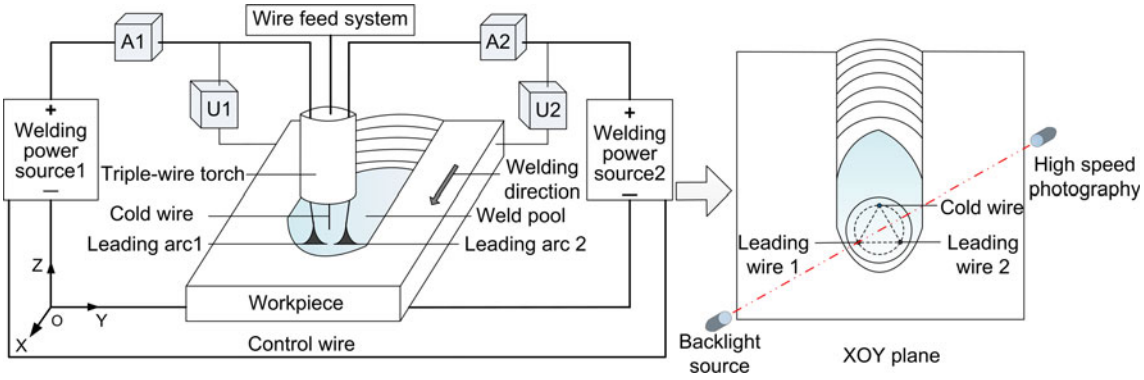

Fig. 2 Experimental system of twin-arc integrated cold wire hybrid welding

pool. The welding direction was perpendicular to the connecting line between the endpoints of two consumable electrodes. According to the positions of wires, the two consumable electrodes were defined as leading wire 1 and leading wire 2, respectively. The third wire was defined as the cold wire, which indicated that there was no arc established between this wire and the workpiece. The two welding power sources were set to the same pulse mode and preset values, as shown in Table 1. Moreover, these welding power sources can output in-phase pulse currents through communication with each other. In this study, the cold wire feed speed was varied from 0.8 to 2.8 m/min while other welding parameters were kept constant. The high-speed photographs for arc behavior and metal transfer process were captured synchronically with the electrical signals to accurately demonstrate the detailed information of the welding process. The capturing rate was 1000 frames per second. The shooting direction was perpendicular to the connecting line between the endpoints of the leading wire 2 and cold wire, and the backlight source was placed behind the leading wire 1. For all the experimental cases, all of the wires were H08Mn2SiA with diameter of 1.2 mm. Bead-on-plate welding were carried out on mild steel at a welding speed of 0.24 m/min. The shielding gas used in this experiment was 85 % Ar+15 % CO_2 with a flow rate of 25 L/min.

3 Results and discussion

3.1 Force analysis of arc

Figure 3 shows the actual arcing situation during the pulse current phase, and the high-speed photograph shows the front projection of three wires in backlight plane, and three wires, in turn, are the leading wire 2, leading wire 1, and cold wire from left to right. When the pulse peak currents were supplied to the two consumable electrodes, the two arcs would deflect towards each other. Both leading arcs 1 and 2 deflected towards each other, and the small parts of two arcs banded together and shared a common conductive zone, which is defined as arc coupling area.

For purpose of better understanding the mutual deflection of arcs, firstly, the simplified force analysis of two arcs were made, as shown in Fig. 4. Although the arc is neutral in macro, it is composed of the positive and negative charges that are always moving in electric field direction to form current in micro. Therefore, the two wires are equivalent to a pair of mutually parallel conductors. It is well known that a pair of conductors supplied with the same direction currents is subjected to the attractive forces. The formation of force is because the current passing through one arc generates the electric magnetic field around the other arc, which makes the arc subjected to the electromagnetic force [20].

The magnetic flux density around the wire 1 inducted by the arc 2, B_1, is

$$B_1 = \frac{\mu_0 I_2}{2\pi D_E} \tag{1}$$

where D_E is the interwire distance, I_2 is the arc 2 current, and μ_0 is the permeability of free space. The electromagnetic force, namely the Lorentz force F_1 induced by the magnetic flux density B_1 with the arc 1 current is

$$F_1 = j_1 \times B_1 \tag{2}$$

where j_1 is the current density of the arc 1 and denoted by $j_1 = I_1/\pi r_1^2$, I_1 is the arc 1 current, and r_1 is the radius of the arc 1 column.

Table 1 Basic welding parameters used in this experiment

Preset current/A	Preset voltage/V	Pulse current/A	Basic current/A	Pulse time/ms	Basic time/ms	Frequency/Hz
180	24	600	100	1.8	6.8	116

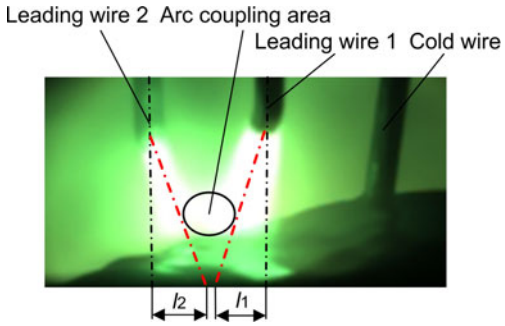

Fig. 3 Actual arcing situation during the pulse current phase

Likewise, the Lorentz force F_2 induced by the magnetic flux density B_2 with the arc 2 current is

$$F_1 = j_2 \times B_2 \tag{3}$$

where B_2 is the magnetic flux density around the wire 2 and denoted by $B_2 = \frac{\mu_0 I_1}{2\pi D_E}$, j_2 is the current density of the arc 2 defined by $j_2 = I_2/\pi r_2^2$, I_2 is the arc 2 current, and r_2 is the radius of the arc 2 column.

The force analysis of two arcs in the *XOY* plane is illustrated in Fig. 5. Both leading arcs 1 and 2 were subjected to electromagnetic forces F_{21} and F_{12}, respectively. Moreover, because the materials and diameters of two wires as well as currents supplied to wires were all the same, F_{12} was equal to F_{21}. The force resolution in shooting direction is shown in Fig. 6. F_{21n} and F_{12n} were component forces that were parallel to shooting direction, respectively. F_{21t} and F_{12t} were component forces that were perpendicular to shooting direction, respectively.

What is shown in Fig. 6 is the force analysis of arc in shooting direction. The electromagnetic force F_{21t} and F_{12t}, respectively, acted on the leading arcs 1 and 2, which resulted in the deflection of arcs towards each other. The deflected distances for the leading arcs 1 and 2 were defined as l_1 and l_2, respectively. Moreover, due to the short interwire distance, the small parts of two arcs banded together and shared a common

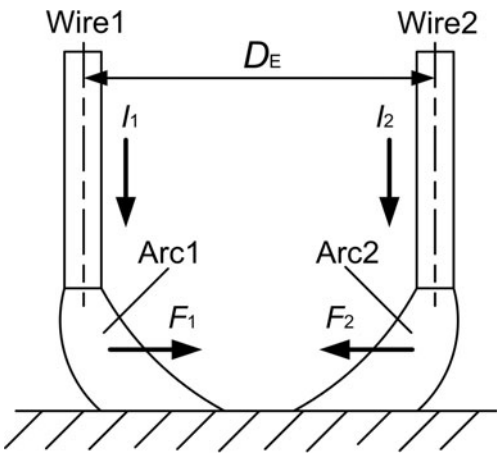

Fig. 4 Force analysis of arc during the pulse current phase

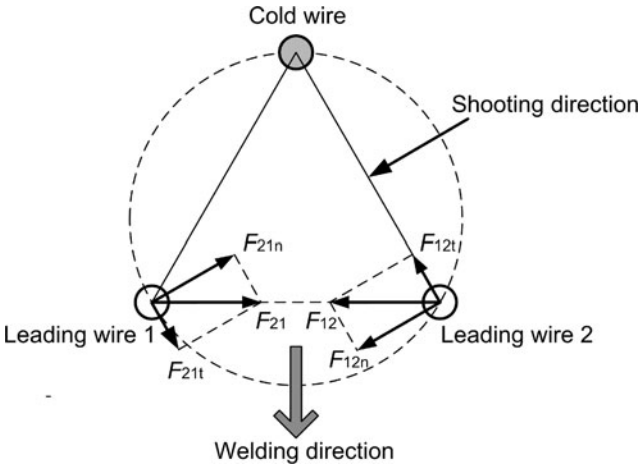

Fig. 5 Force analysis of arc in *XOY* plane

conductive zone, i.e., arc coupling area, as shown in shaded area.

3.2 Effect of cold wire on welding stability

The twin-arc integrated cold wire hybrid welding was characterized by increasing the deposition rate while the heat input kept constant. In addition, the cold wire in this triple-wire arc welding has the potential function that is stabilizing the cathode spots to improve the welding stability. Through a great many experiments about varying the cold wire feed speeds, the statuses of the cold wire were divided into four categories: separated from the weld pool, contacting superficially with the top layer of the weld pool, deeply inserting into the liquid weld pool, and insufficiently melted. The reason to distinguish between superficially and deeply inserting into the weld pool was that the welding stability could be significantly improved when the cold wire tip was sufficiently inserted into the liquid

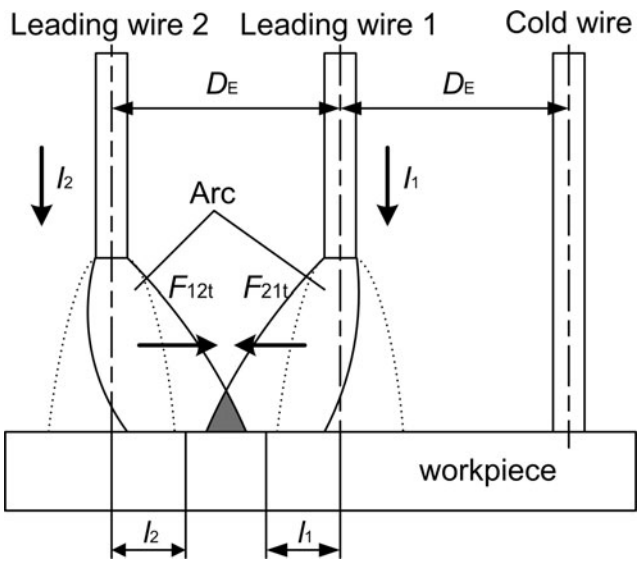

Fig. 6 Force analysis of arc in shooting direction

weld pool. Because the last status of cold wire (insufficiently melted) obviously deteriorated the welding stability, the only first three statuses of cold wire were selected to study in this experiment. Therefore, the electrical signals and high-speed photographs of the welding process for cold wire feed speeds of 1.2, 1.8, and 2.4 m/min were taken to demonstrate the above three characteristic statuses, respectively. The basic welding parameters used in the experiments are presented in Table 1 except in instances where other values are explicitly stated.

Figure 7 shows the high-speed photographs with corresponding electrical signals at the cold wire feed speed of 1.2 m/min. At this moment, the cold wire stayed at the status of separated from the weld pool, and the metal transfer mode was projected spray instead of streaming spray. Supplied by in-phase currents, both the leading wires 1 and 2 kept arcing simultaneously. This arcing mode made the two wires to be heated and melted by mutual arcs, which resulted in the arc length more longer than which of a single wire arcing at the same welding parameters. Moreover, the two arcs deflected towards each other, which changed the direction of arc force acting on the droplet. Thus, the metal transfer mode was projected spray rather than streaming spray at a peak current about 600 A for a filler wire of 1.2 mm. During the base current phase at 654 ms, as indicated with arrows in Fig. 7, the cathode spot was located below the tip of the leading wire 2. During the initial pulse current phase at 657 ms, the arc extremely bright zones appeared on the fresh surfaces of two wire tips, and it was too late for the arc extremely bright zones to expand to arrange in bundles. In addition, the small parts of two arcs banded together and shared a common conductive zone, i.e., arc coupling area, where the cathode spot was located on the surface of the weld pool. The arc coupling area was more conductive to maintaining a stable arc conductive channel because the cathode spot was capable of seeking zone with lower electronic work function. From 664 to 666 ms, the cathode spot has moved to the right of the leading wire 2 with the rear flow of the surfacing liquid weld pool metal. From 673 to 692 ms, the cathode spot moved from the right of the leading wire 2 to the center between the tips of the leading wires 1 and 2. The location of the arc coupling area varied with the movement of the cathode spot, which would cause the deflection of the leading arcs 1 and 2 relative to the respective wire axis.

At the moment of 698 ms, the cathode spot was located at the center between the tips of the leading wires 1 and 2, but it moved to the left of leading wire 1 at 708 ms. The comparison of the arc shapes between 700 and 718 ms showed that the arc coupling area moved to the right with the greater deflected distance of leading arc 2 and the less deflected distance of

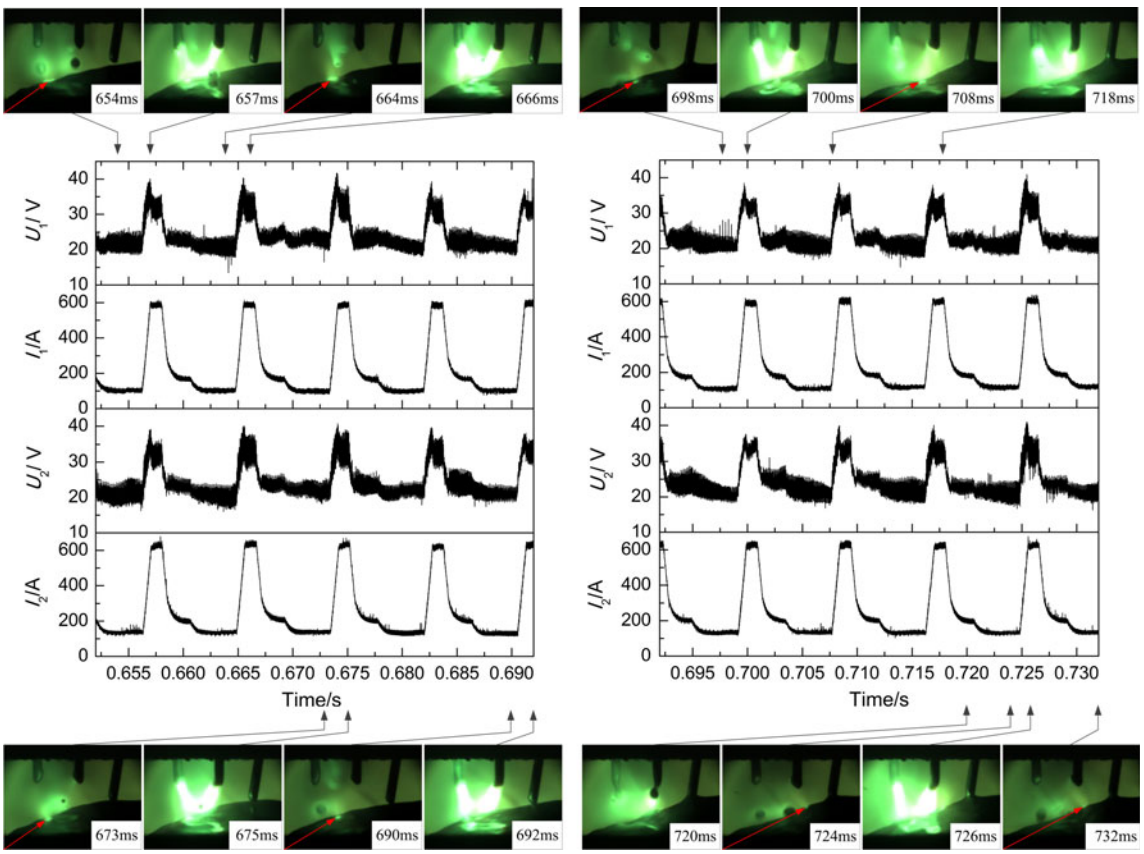

Fig. 7 Arcing situation at the cold wire feed speed of 1.2 m/min

leading arc 1. At 720 ms, the necking formed between the tips of two molten wires and the droplets, and the droplets detached from the wire tips and transferred towards the weld pool at 724 ms. From 724 to 732 ms, the cathode spot has moved behind the leading wire 1.

The cathode spot drifted with the rear flow of the liquid weld pool metal when the cold wire was separated from the weld pool. This led to significant location variations of the arc coupling area and deflected distance variations of the leading arcs 1 and 2, which all deteriorated the welding process stability.

Figure 8 shows the high-speed photographs with corresponding electrical signals at the cold wire feed speed of 1.8 m/min. In this case, the cold wire was not separated from the weld pool, but contacted superficially with the top layer of the weld pool. Although the movement of cathode spot was not observed, the location of the arc coupling area as well as deflected distances of two arcs varied obviously. At the moment of 208 ms, the droplets detached from tips of two molten wires and transferred towards the weld pool. At 211 ms, the leading arc 1 deflected obviously to the left while the leading arc 2 barely deflected, which caused the location of the arc coupling area to be closer to the leading wire 2. At 214 ms, the droplets detached from tips of the leading wires 1 and 2 with the end of the pulse currents. From 216 to 218 ms, the arc extremely bright zones disappeared gradually with the separation of two arcs from each other. However, with the pulse currents once again supplied to the wires at 219 ms, the leading arc 2 deflected to the right obviously, and the arc coupling area moved closer to the leading wire 1. At 224 ms, the droplets detached from tips of the leading wires 1 and 2 with the end of pulse currents.

The comparison of arc shapes between 237 and 245 ms showed that the arc coupling area moved from below the tip of the leading wire 2 to the center between the tips of the leading wires 1 and 2. With pulse currents continuing to be supplied, two arcs expanded as cone shapes to increase the area of common conductive zone at the moment of 246 ms. During the base current phase from 249 to 251 ms, the arc extremely bright zones disappeared gradually with the separation of two arcs from each other. During the initial pulse current phase at 253 ms, it was observed that the faint plasma of the leading arc 2 suddenly deflected to the right, and the arc coupling area moved closer to the leading wire 1 at 254 ms. The movement of the arc coupling area to the right was observed obviously from 235 to 254 ms.

Although the movement of cathode spot was not observed, the deflected distances of two arcs varied obviously, that is, the deflected distance of the leading arc 2 increased as the deflected distance of the leading arc 1 decreased. This led to

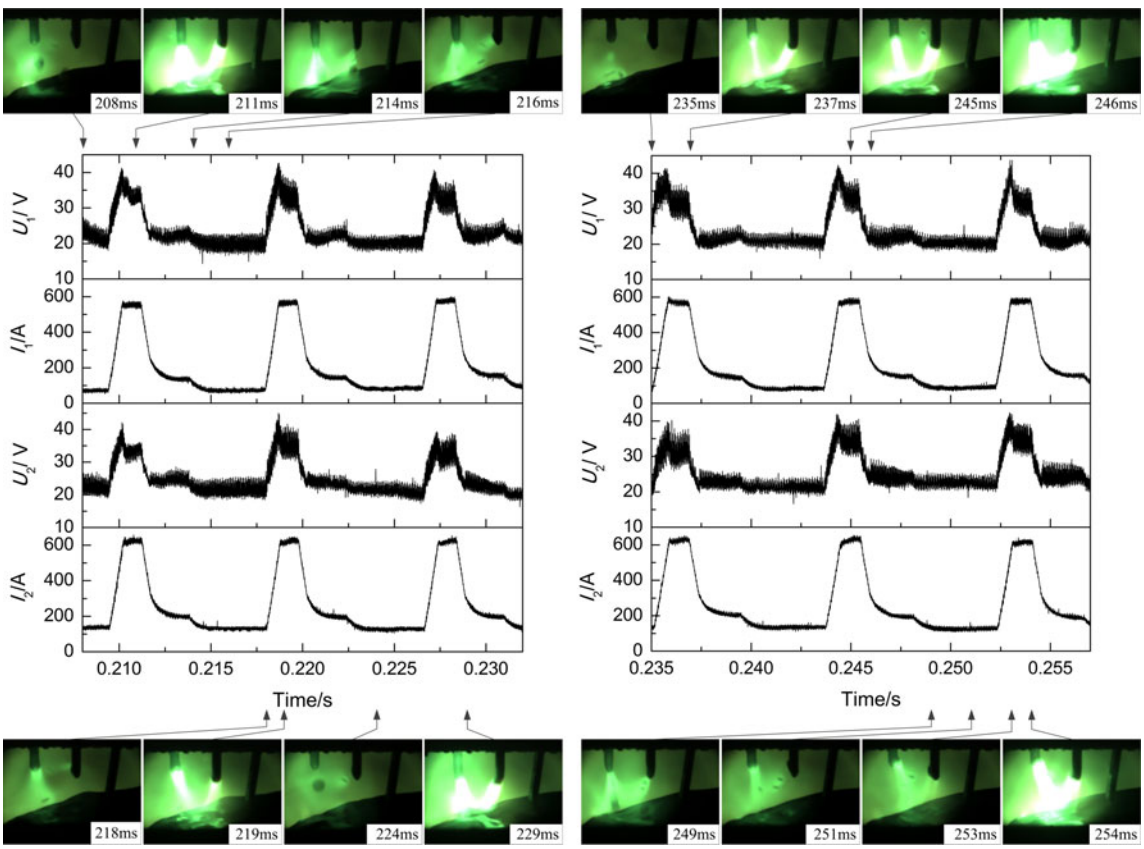

Fig. 8 Arcing situation at the cold wire feed speed of 1.8 m/min

significant location movement of the arc coupling area to the right, which deteriorated the welding process stability.

Figure 9 shows the high-speed photographs with corresponding electrical signals at the cold wire feed speed of 2.4 m/min. In this case, the cold wire was further inserted into the weld pool. It was observed that the arc coupling area was stabilized in the same position without moving with the rear flow of the liquid weld pool metal. At the same time, the deflected distances of two arcs had little variation, and the welding process was very stable. During the base current phase at 3189 ms, the arc plasma was hardly observed. At 3191 ms, with the pulse currents supplied to the wires, double arcs started to ignite simultaneously and deflected towards each other to form the arc coupling area. The arc coupling area was located at the center between the tips of the leading wires 1 and 2. At 3193 ms, the arc extremely bright zones disappeared gradually with the end of pulse currents, and the necking formed between the tips of two molten wires and the droplets. At 3195 ms, the droplets detached from the wire tips and transferred towards the weld pool under the action of electromagnetic force and plasma flow force. Besides, the above process was repeated in the pulse period, as shown in the high-speed photographs from 3200 to 3234 ms. The comparison of arcing situations during the pulse current phase (at 3191, 3200, 3209, 3217, 3226, and 3234 ms) showed that the arc coupling area was stabilized in the same position without any movement, and the deflected distances of two arcs also kept constant values. Hence, there was no fluctuation of arc lengths, which contributed to welding process stability.

Based on the above phenomena, it is demonstrated that the cathode spot (arc coupling area) can be stabilized to reduce the deflected distances of two arcs and improve the welding stability when the cold wire feed speed is in a proper range. The main reasons are as follows:

(1) Firstly, the formation of cathode spot is provided with conditions of electron emission that are mainly thermionic emission and field emission. Secondly, the cathode spot is capable of seeking zone with lower electronic work function, and higher temperature is more conductive to the electron emission [21]. Finally, because of the addition of cold wire, the temperature of the liquid weld pool metal around the cold wire was decreased significantly, which increased the difficulty of the electron emission. Thus, the cathode spot would choose to stabilize in higher temperature zone instead of moving with the rear flow of the liquid weld pool metal.
(2) The uneven temperature distribution of the weld pool results in surface tension variation, and the liquid weld pool metal flows in direction from low surface tension

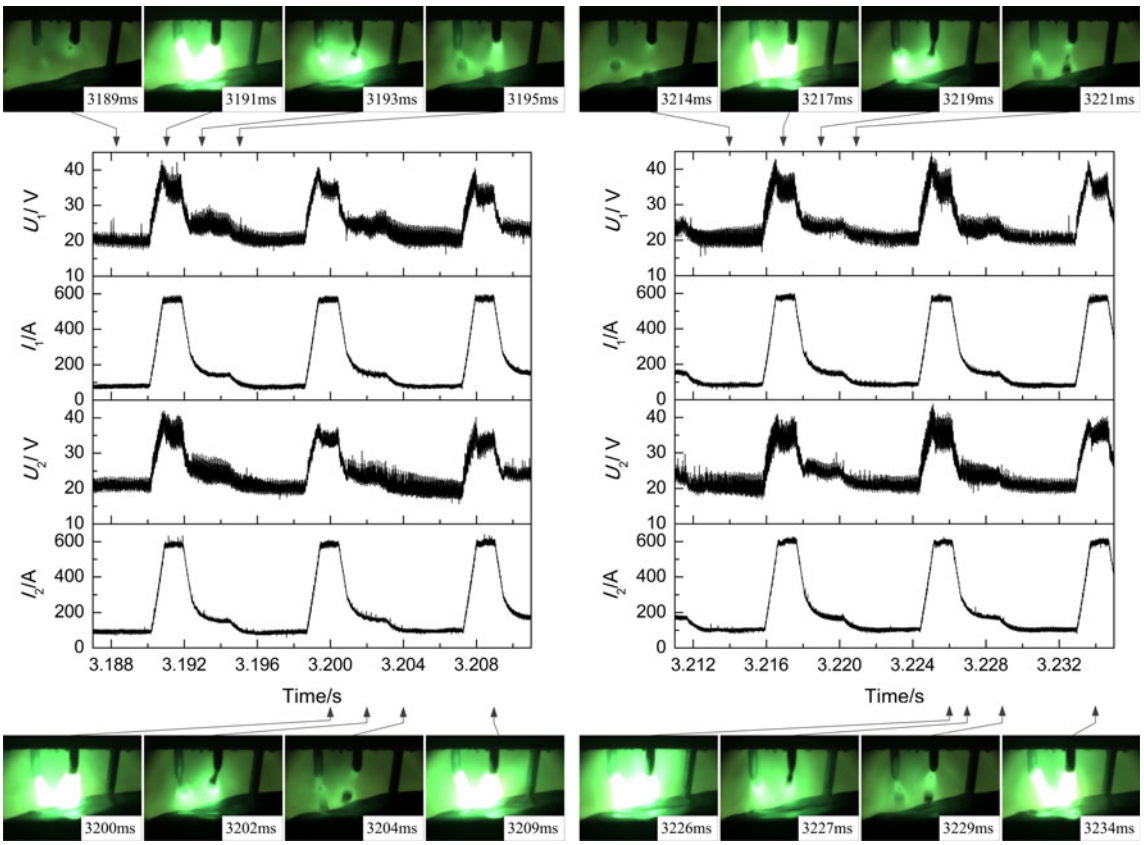

Fig. 9 Arcing situation at the cold wire feed speed of 2.4 m/min

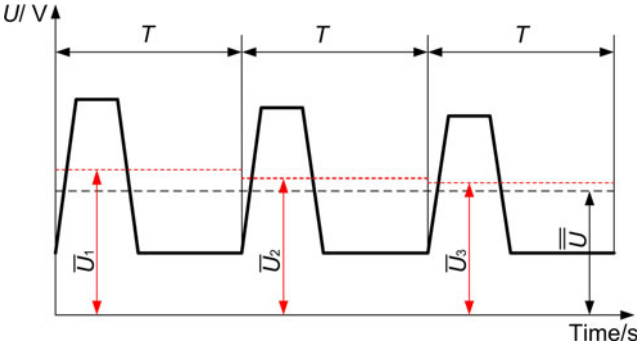

Fig. 10 Schematic diagram of the statistical method

(high temperature) to high surface tension (low temperature) [22–24]. Moreover, in practical welding, the cold wire was fed into the head zone of the weld pool rather than in the trailing zone of the weld pool because three wires were integrated closely in a single weld torch. Thus, the addition of cold wire mainly decreased the head zone temperature of the weld pool rather than the trailing zone temperature of the weld pool, which could reduce gradient distribution of surface tension to slow down the flow of the liquid weld pool metal. Consequently, the cathode spot could be stabilized.

(3) The addition of cold wire can slow down the turbulently rolling weld pool caused by high energy input, which contributed to calm down the flow of the liquid weld pool metal. So to some extent, the smooth flow of the liquid weld pool metal was also conductive to stabilizing the cathode spot.

3.3 Quantitative analysis of welding stability

In order to verify the above conclusions, the electrical signals were analyzed by mathematical methods. Thus, welding process stability under the above three cold wire feed speeds was analyzed by the mathematical statistics method.

The mean value (arithmetic mean) that is the index of data central tendency represents the average of a sample, which is denoted by

$$\overline{X} = \frac{1}{n}\sum_{i=1}^{n} X_i \tag{4}$$

where $\overline{X}$ is the sample mean, n is the sample size, and X_i is the variable value.

The variance describes the deviation degree between random variables and mean value, which is denoted by

$$S^2 = \frac{1}{n-1}\sum_{i=1}^{n}\left(X_i - \overline{X}\right)^2 \tag{5}$$

where S^2 is the sample variance.

The arc is composed of the three sections characterized by different electric field intensities, i.e., the anode region, cathode region, and arc column region. In addition, the arc voltage is the sum of the voltage drop of the above three regions, denoted by

$$U = U_{\mathrm{A}} + U_{\mathrm{C}} + U_{\mathrm{P}} \tag{6}$$

$$U_{\mathrm{P}} = EL \tag{7}$$

where U is the arc voltage, U_{A} is the anode voltage drop, U_{P} is arc column voltage drop, U_{C} is the cathode voltage drop, E is the electric field intensity of arc column, and L is the arc length.

Thus, it can be seen that the arc voltage is proportional to the arc length, and the welding stability is evaluated by the fluctuation of arc length. Therefore, the welding stability can be evaluated by the fluctuation of arc voltage. Moreover, the less variance of arc voltage is, the more stable welding process will be. Whereas the greater variance of arc voltage is, the less stable welding process will be.

The schematic diagram of this method is shown in Fig. 10. This method was divided into three steps. Firstly, the average voltages ($\overline{U}_1\overline{U}_2\overline{U}_3$) in several pulse periods were chosen as a set of variables used to calculate the deviation from the overall

Table 3 Results of hypothesis test for leading arc 1

Arc 1	α	$S^2_{\overline{U}_1}$	$F = \frac{S^2_{\overline{U}_{1(2)}}}{S^2_{\overline{U}_3}}$
v_c=1.2 m/min	0.01	0.60604	6.00337
v_c=2.4 m/min		0.10095	
v_c=1.8 m/min	0.01	0.72174	7.14948
v_c=2.4 m/min		0.10095	

Table 2 Results of arc voltage statistical parameters

	Serial number	Number	$\overline{\overline{U_1}}$	$\overline{\overline{U_2}}$	$S^2_{\overline{U}_1}$	$S^2_{\overline{U}_2}$
v_c=1.2 m/min	1	11	24.50102	24.70244	0.60604	0.62449
v_c=1.8 m/min	2	11	24.88119	24.63462	0.72174	0.79063
v_c=2.4 m/min	3	12	24.59755	24.88243	0.10095	0.09551

Table 4 Results of hypothesis test for leading arc 2

Arc 2	α	$S^2_{\overline{U}_2}$	$F=\frac{S^2_{\overline{U}_{1(2)}}}{S^2_{\overline{U}_3}}$
v_c=1.2 m/min	0.01	0.62449	6.53848
v_c=2.4 m/min		0.09551	
v_c=1.8 m/min	0.01	0.79063	8.27798
v_c=2.4 m/min		0.09551	

average voltage ($\overline{\overline{U}}$). Secondly, the comparison among the variances of three cold wire feed speeds was made by means of the parametric hypothesis test. Finally, the judgment was made between the null hypothesis and alternative hypothesis.

What is seen in Table 2 are the results for the statistical parameters of arc voltage corresponding to the cold wire feed speeds of 1.2, 1.8, and 2.4 m/min, respectively. Where v_c represents for the cold wire feed speed, and n is the sample size to represent for the number of random variables. $\overline{\overline{U_1}}$ and $\overline{\overline{U_2}}$ are the overall average voltages for the leading arcs 1 and 2, respectively. $S^2_{\overline{U}_1}$ and $S^2_{\overline{U}_2}$ are the variances for the leading arcs 1 and 2, respectively, which represent for the fluctuation between the average voltage of each pulse period and the overall average voltage. The evaluation of welding stability comes down to the variance comparison under three cold wire feed speeds.

Compared among the sample variances under three cold wire feed speeds, it was seen that the welding stability was significantly improved with the increase of cold wire feed speed to an appropriate value (0.60604>0.10095, 0.62449>0.095511, 0.72174>0.10095, 0.79063>0.095511). However, the variances of continuously several pulse periods were randomly selected as a set of sample, which could not represent the whole welding process stability. Therefore, the stability judgment of the whole welding process based on the sample observations can be realized by a method of hypothesis test [25].

The distribution of average voltage $\overline{U}$ follows a normal distribution $N(\mu, \sigma^2)$. The hypothesis test is put forward as follows:

$$H_0:\sigma_1^2=\sigma_3^2 \leftrightarrow H_1:\sigma_1^2>\sigma_3^2 \text{ or } H_0:\sigma_2^2=\sigma_3^2 \leftrightarrow H_1:\sigma_2^2>\sigma_3^2$$

Because the μ_1 and μ_3 are unknown, the Fisher test is chosen to use as follows:

$$F=\frac{S_1{}^2}{S_3^2}\sim F(n_1-1,n_3-1) \text{ or } F=\frac{S_2{}^2}{S_3^2}\sim F(n_2-1,n_3-1)$$

where μ and σ^2 are the mean and variance of normal distribution, respectively. $\sigma_1{}^2$, $S_1{}^2$, and n_1 are the population variance, sample variance, and sample size at the cold wire speed of 1.2 m/min, respectively. Likewise, $\sigma_2{}^2$, $S_2{}^2$, and n_2 are the corresponding statistical parameters at the cold wire speed of 1.8 m/min; $\sigma_3{}^2$, $S_3{}^2$, and n_3 are also the corresponding statistical parameters at the cold wire speed of 2.4 m/min.

The corresponding results of hypothesis test for the leading arc 1 are shown in Table 3. The significance level α was selected as 0.01, and $F_{0.99}$ (10, 11) is equal to 4.54, which is obtained from the Fisher distribution quantile table. The Fisher test value 6.00337 and 7.14948 are greater than 4.54 for the comparison between the cold wire feed speeds of 1.2 and 2.4 m/min or 1.8 and 2.4 m/min. Therefore, the null hypothesis was rejected, and the alternative hypothesis was accepted. Under confidence level of 0.99, it was proved that the welding stability at the cold wire feed speed of 2.4 m/min was better than the welding stability at the cold wire feed speed of 1.2 and 1.8 m/min.

Similarly, the corresponding results of hypothesis test for the leading arc 2 are shown in Table 4. The significance level α was selected as 0.01, and $F_{0.99}$ (10, 11) is equal to 4.54. Likewise, The Fisher value 6.53848 and 8.27798 are greater than 4.54 for the comparison between the cold wire feed speeds of 1.2 and 2.4 m/min or 1.8 and 2.4 m/min. Therefore, the null hypothesis was rejected, and the alternative hypothesis was accepted. Under confidence level of 0.99, it was proved that the welding stability at the cold wire feed speed of 2.4 m/min was better than the welding stability at the cold wire feed speed of 1.2 and 1.8 m/min.

In conclusion, by means of hypothesis test, it was fully verified that the welding stability was improved with the increase of cold wire feed speed to an appropriate value.

3.4 The relationship between the cold wire feed speed and its status in weld pool

What is shown in Fig. 11 is the corresponding relationship between the cold wire feed speed and its status in the weld pool. The cold wire stayed at the status of separated from the weld pool or the critical state of contacting the weld pool surface when the cold wire speed was less than 1.6 m/min. The cold wire contacted superficially with the top layer of the weld pool when the cold wire feed speed increased to between 1.6 and 2.2 m/min. When the cold wire feed speed was between 2.2 and 2.6 m/min, the cold wire was deeply inserted

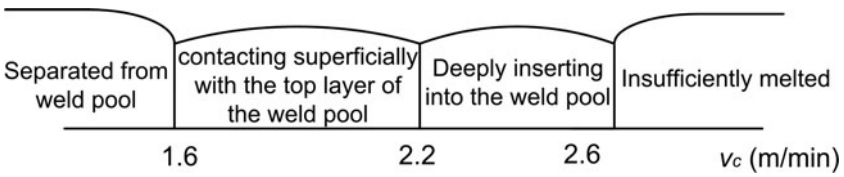

Fig. 11 Corresponding relationship between the cold wire feed speed and its status

into the liquid weld pool. In addition, the welding stability could be significantly improved in this range from 2.2 to 2.6 m/min. When the cold wire feed speed was more than 2.6 m/min, the cold wire could not be sufficiently melted. Consequently, it would sway inside the weld pool along the welding direction or even in random directions, which deteriorated the welding process stability. Besides, with the increase of cold wire feed speed from 0.8 to 2.6 m/min, the deposition rate would increase from 6.642 to 7.476 kg/h, but the dilution would decrease from 33.81 to 25.44 %.

4 Conclusions

A novel high-efficient welding technology entitled twin-arc integrated cold wire hybrid welding was developed. The welding process was monitored by the high-speed photography and electrical signal acquisition synchronously. What is more important, the significant effect of the cold wire on welding stability was studied to draw the following conclusion:

(1) In addition of increasing deposition rate, the cold wire played an important role in improving the welding stability. The addition of cold wire could stabilize the cathode spot on the surface of the weld pool without drifting with the rear flow of the liquid weld pool metal, which all contributed to decreasing the fluctuation of arc length and improving the welding stability.
(2) The welding stability was evaluated by the fluctuation of arc voltage, and the welding stability at different cold wire feed speeds was compared by the hypothesis test. In this way, it was fully verified that the welding process was more stable with the increase of cold wire feed speed to a proper range.
(3) On the condition of the welding system in this paper, the cold wire stayed at the status of separated from the weld pool or the critical state of contacting the weld pool surface when the cold wire speed was less than 1.6 m/min. The cold wire contacted superficially with the top layer of the weld pool when the cold wire feed speed increased to between 1.6 and 2.2 m/min. When the cold wire feed speed was between 2.2 and 2.6 m/min, the cold wire was deeply inserted into the liquid weld pool. In addition, the welding stability could be significantly improved in this range. When the cold wire feed speed was more than 2.6 m/min, the cold wire could not be sufficiently melted.

Acknowledgments This research work was funded by the National Natural Science Foundation of China (grant no. 51475325), the Applied Foundation and Advanced Technology Research Planning Project of Tianjin (grant no. 14JCYBJC19100).

Conflict of interest The authors declare that they have no competing interests.

References

1. Kah P, Suoranta R, Martikainen J (2012) Advanced gas metal arc welding processes. Int J Adv Manuf Technol 67(1-4):655–674
2. Layus P, Kah P, Martikainen J, Gezha VV, Bishokov RV (2014) Multi-wire SAW of 640 MPa Arctic shipbuilding steel plates. Int J Adv Manuf Technol 75(5-8):771–782
3. Li KH, Zhang YM, Xu P, Yang FQ (2008) High-strength steel welding with consumable double-electrode gas metal arc welding. Weld J 87(3):57S–64S
4. Yang X, Xu Q, Yin N, Xiao X (2011) Twin-wire submerged arc welding process of a high-strength low-alloy steel. J Wuhan Univ Technol 26(1):114–117
5. Yan CY, Huang JC, Wang L, Zhu D, Yang SZ, He SM (2013) Influence of welding-parameters on weld appearance and mechanical properties in twin-wire tandem submerged arc welding of HSLA steel. Adv Mater Res 735–755:358–362
6. Ueyama T, Ohnawa T, Tanaka M, Nakata K (2005) Effects of torch configuration and welding current on weld bead formation in high speed tandem pulsed gas metal arc welding of steel sheets. Sci Technol Weld Join 10(6):750–759
7. Moinuddin SQ, Sharma A (2015) Arc stability and its impact on weld properties and microstructure in anti-phase synchronised synergic-pulsed twin-wire gas metal arc welding. Mater Des 67:293–302
8. Zhang YM, Jiang M, Lu W (2004) Double electrodes improve GMAW heat input control. Weld J 83(11):39–41
9. Wu CS, Hu ZH, Zhong LM (2012) Prevention of humping bead associated with high welding speed by double-electrode gas metal arc welding. Int J Adv Manuf Technol 63(5-8):573–581
10. Li KH, Chen JS, Zhang YM (2007) Double-electrode GMAW process and control. Weld J 86(8):231S–237S
11. Wu CS, Zhang MX, Li KH, Zhang YM (2007) Numerical analysis of double electrode gas metal arc welding process. Comp Mater Sci 39(2):416–423
12. Ribic B, Palmer TA, DebRoy T (2009) Problems and issues in laser-arc hybrid welding. Int Mater Rev 54(4):223–244
13. Hu B, den Ouden G (2005) Synergetic effects of hybrid laser/arc welding. Sci Technol Weld Join 10(4):427–431
14. Wei HL, Li H, Yang LJ, Gao Y, Ding XP (2015) Arc characteristics and metal transfer process of hybrid laser double GMA welding. Int J Adv Manuf Technol 77(5-8):1019–1028
15. Abhay S, Navneet A, Bhanu KM (2008) Mathematical modeling of flux consumption during twin-wire welding. Int J Adv Manuf Technol 38(11-12):1114–1124
16. Bajcer B, Hrzenjak M, Pompe K, Jez B (2007) Improvement of energy and materials efficiencies by introducing multiple-wire welding. Metalurgija 46(1):47–52
17. Yokota Y, Shimizu H, Nagaoka S, Ito K, Arita H (2012) Development and application of the 3-electrode MAG high-speed horizontal fillet welding process. Weld World 56(1-2):43–47
18. Arita H, Morimoto T, Nagaoka S, Nakano T (2009) Development of advanced 3-electrode MAG high-speed horizontal fillet welding process. Weld World 53(5-6):35–43
19. Raudsepp H (2015) integrated cold electrode—latest advancement in submerged arc welding. Electr Weld Mach 45(5):28–32
20. Ueyama T, Ohnawa T, Tanaka M, Nakata K (2007) Occurrence of arc interaction in tandem pulsed gas metal arc welding. Sci Technol Weld Join 12(6):523–529
21. Zhou X, Heberlein J, Pfender E (1994) Theoretical study of factors influencing arc erosion of cathode. IEEE Trans Components Packaging Manuf Technol 17(1):107–112

22. Zhang W, Roy GG, Elmer JW, DebRoy T (2003) Modeling of heat transfer and fluid flow during gas tungsten arc spot welding of low carbon steel. J Appl Phys 93(5):3022–3033
23. Patankar SV (1980) Numerical heat transfer and fluid flow. Hemisphere Publishing Corporation, Washington D.C
24. Cho DW, Kiran DV, Song WH, Na SJ (2014) Molten pool behavior in the tandem submerged arc welding process. J Mater Process Technol 214(11):2233–2247
25. Shi DJ, Zhang YH (2008) Applied mathematical statistics. Tianjin University Press, Tian Jin